Article:
Capel Berdiell, I, Kulmaczewski, R, Warriner, SL et al. (2020) Iron and Silver Complexes of 4-(Imidazol-1-yl)-2,6-di(pyrazol-1-yl)-pyridine (L), Including a [Fe3(μ-F)2F6L8]+ Assembly. European Journal of Inorganic Chemistry, 2020 (46). pp. 4334-4340. ISSN: 1434-1948

https://doi.org/10.1002/ejic.202000782

Iron and Silver Complexes of 4-(Imidazol-1-yl)-2,6-di(pyrazol-1-yl)-pyridine (*L*), Including a $[Fe_3(\mu\text{-}F)_2F_6L_8]^+$ Assembly

Izar Capel Berdiell,[a,b] Rafal Kulmaczewski,[a] Stuart L. Warriner,[a] Oscar Cespedes[c] and Malcolm A Halcrow*[a]

Abstract: Treatment of 2,4,6-trifluoropyridine with sodium imidazolate, then 2 equiv sodium pyrazolate, in two reaction steps yields the title ligand *L* in 40 % overall yield. Crystalline $[FeL_2][BF_4]_2$ and $[FeL_2][ClO_4]_2$ are isostructural high-spin complexes, with highly twisted six-coordinate geometries and pendant imidazolyl groups. Conversely, $[Ag(\mu\text{-}L)]BF_4\cdot\frac{1}{2}MeCN$ is a linear coordination polymer of distorted square planar silver ions linked by $\kappa^1{:}\kappa^3,\mu\text{-}L$ ligands. Some samples of $[FeL_2][BF_4]_2$ were contaminated by $[Fe^{III}_3(\mu\text{-}F)_2F_6L_8]BF_4$, which was prepared in pure form following reaction of $Fe[BF_4]_2\cdot 6H_2O$, $Na_3[FeF_6]$ and *L* in appropriate ratios. The linear $[\{trans\text{-}FeFL_4\}_2(\mu\text{-}F)_2FeF_4]^+$ assembly is supported by monodentate *L* ligands coordinated through their imidazolyl donors, and donating C−H...F interactions to the central $[FeF_6]^{3-}$ moiety. The cluster exhibits moderate antiferromagnetic coupling between its iron(III) centers.

Introduction

2,6-Di(pyrazol-1-yl)pyridine (bpp or 1-bpp[1]) and its derivatives are an important group of tridentate "terpyridine analogue" ligands (Scheme 1).[2-5] Their synthetic flexibility is a particular advantage of the bpp ligand family, which can be derivatized at every position of the ligand skeleton using available starting materials, easily synthesized pyrazole precursors and/or straightforward functional group transformations. They have found particular use as components in iron(II) spin-crossover materials, where over 100 complex salts of different $[Fe(bpp)_2]^{2+}$ derivatives are now available.[3,4] As well as providing a unique library for structure:function studies,[3,6-8] bpp derivatives bearing conductive, fluorescent, photoswitchable or tether substituents have proven very useful for multifunctional spin-crossover compounds.[9,10] An useful family of lanthanide photosensitizer ligands for biological imaging is based on the bpp ligand scaffold,[2,11] while bpp derivatives have also proven useful for catalysis[12-14] and as components in dye-sensitized solar cells.[15]

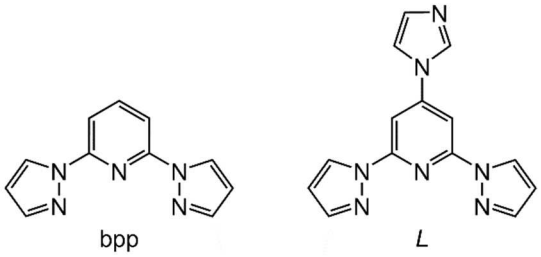

Scheme 1. The prototypical bpp ligand, and its new derivative *L*.

We recently reported that addition of silver salts to solutions of preformed $[M(tpt)_2]^{2+}$ (M = Fe, Co, Ni; tpt = 2,4,6-tri(pyrazol-1-yl)-1,3,5-triazine) yields thixotropic, heterometallic coordination polymer gels.[16] Solution studies and crystal structures of model compounds imply the gels are formed from $[\{MAg(\mu\text{-}tpt)_2\}_n]^{3n+}$ assemblies, with alternating M^{2+} and Ag^+ ions linked by ditopic tpt ligands. Given our on-going interest in spin-crossover materials,[3] we have also screened other ditopic di- or tri-(pyrazolyl)azines as bridging ligands in assembly structures (or gels) with spin-crossover switching properties.[16-19] Continuing this effort, we now report the ditopic ligand 4-(imidazol-1-yl)-2,6-di(pyrazol-1-yl)pyridine (*L*, Scheme 1), a potentially bridging ligand with divergent tridentate and monodentate metal-binding domains,[5] and its iron and silver complexes. Our results include the unexpected isolation of an unusual $[Fe_3(\mu\text{-}F)_2F_6L_8]^+$ complex, with a linear $[Fe^{III}_2(\mu\text{-}F)_2Fe^{III}F_4)]^{3+}$ core supported by monodentate *L* coordination.

Results and Discussion

Substitution of the fluoro groups in 2,4,6-trifluoropyridines by amine nucleophiles occurs preferentially at the *C*4 position.[20] Thus, 2,6-difluoro-4-(imidazol-1-yl)pyridine was prepared in moderate yields by treatment of sodium imidazolate with excess 2,4,6-trifluoropyridine (to reduce byproducts from multiple substitution). Reaction of this purified intermediate with 2 equiv sodium pyrazolate under the same conditions yielded *L*, in an overall yield of 40 % over the two steps. The identity of both compounds was confirmed crystallographically. 2,6-Difluoro-4-(imidazol-1-yl)pyridine (monoclinic, space group *Pc*, *Z* = 12) is notable as a high-*Z'* crystal, with six independent molecules of the

[a] Dr. I Capel Berdiell, Dr. R. Kulmaczewski, Dr. S. L. Warriner, Prof M. A. Halcrow
School of Chemistry
University of Leeds
Woodhouse Lane, Leeds, UK LS2 9JT.
m.a.halcrow@leeds.ac.uk.
[b] Dr. I Capel Berdiell, current address:
Institute of Electronic Structure and Laser,
Foundation for Research and Technology - Hellas,
P.O. Box 1527, GR-711 10 Heraklion, Greece.
[b] Dr. O. Cespedes
School of Physics and Astronomy
University of Leeds
EC Stoner Building, Leeds, UK LS2 9JT.

compound in its asymmetric unit (Figure S3).[21] Two polymorphs of *L* were isolated; the α-polymorph (orthorhombic, *Pna*2_1, Z = 8) contains two crystallographically independent molecules, but the unique half-molecule in β-*L* (orthorhombic, *Pnma*, Z = 4) exhibits whole-molecule disorder across a crystallographic mirror plane which limits the quality of its refinement (Figures S4-S6).

Reaction of silver salts with 1 equiv *L* yields white precipitates, which are insoluble in all common solvents except acetonitrile. Very slow evaporation of an acetonitrile solution of the BF_4^- salt of this compound yielded a few single crystals of a coordination polymer, *catena*-[Ag(μ-*L*)]BF_4·½MeCN (triclinic, $P\bar{1}$, Z = 4). The asymmetric unit of this crystal contains two formula units of the complex. Each silver ion is coordinated by two *L* ligands, one in tridentate fashion with the other being monodentate through its pendant imidazolyl donor (Figure 1). The two silver ions adopt similarly distorted square-planar coordination geometries, with Ag−N bonds ranging from 2.180(6)-2.579(7) Å and a *trans*-N{pyridyl}−Ag−N{imidazolyl} angle of 162.6(2)-164.9(2)°. Such distortions often occur in square planar silver(I) complexes.[22] The main difference between the unique [Ag*L*]$^+$ fragments is the dihedral angle between their pyridyl and imidazolyl groups, which is 28.5(3)° for ligand N(3)-C(23) and 15.3(4)° for ligand N(24)-C(44).

The Ag(1) and Ag(2) sites alternate within the polymer chains, which propagate along the crystallographic (1$\bar{1}$1) vector (Figure S8). Nearest neighbor chains related by crystallographic inversion symmetry are linked by an argentophilic interaction Ag(2)...Ag(2^i) = 3.1728(13) Å[23] (Figure 1; the corresponding distance Ag(1)...Ag(1^{ii}) is longer at 3.6206(14) Å). This places the pyridyl group bound to Ag(2) and the imidazolyl donor to Ag(1^i) in π...π contact; the least squares planes of these groups are separated by 3.40(3) Å, with a dihedral angle of 9.2(5)°.

Crystals of [Ag(μ-*L*)]BF_4·½MeCN decompose on exposure to air, affording a white solid analysing approximately as [Ag(μ-*L*)]BF_4·½H_2O. Electrospray mass spectra of the compound from MeCN solution contain strong [Ag*L*]$^+$ and [AgL_2]$^+$ molecular ions, with no higher nuclearity species being present. That is often found in mass spectra of silver/*N*-heterocyclic ligand assemblies, which are usually labile in solution.[17,18,24]

Isostructural [FeL_2][BF_4]$_2$ and [FeL_2][ClO_4]$_2$ (monoclinic, *C*2/*c*, Z = 4) contain a C_2-symmetric complex cation, with a strongly distorted coordination geometry that is often found in high-spin [Fe(bpp)$_2$]$^{2+}$ derivatives (Figure 2, Table S3).[3,25] The deviation of the molecule from its idealized D_{2d} symmetry is expressed by two parameters: the *trans*-N{pyridyl}−Fe−N{pyridyl} angle (ϕ) and the dihedral angle between the least squares planes of the heterocyclic cores fo the two ligands (θ).[26] High-spin complexes deviating strongly from the ideal values of ϕ = 180° and θ = 90° rarely exhibit thermal spin-crossover, being kinetically trapped in their high-spin form by their rigid crystal lattice.[26,27] The geometries of [FeL_2][BF_4]$_2$ (ϕ = 151.26(9)°, θ = 68.28(2)°) and [FeL_2][ClO_4]$_2$ (ϕ = 151.5(2)°, θ = 68.41(4)°) fall within the range where only high-spin materials are expected (Figure S10). The dihedral angles between the pyridyl and pendant imidazolyl rings in [FeL_2][BF_4]$_2$ and [FeL_2][ClO_4]$_2$ are 8.12(13) and 7.6(3)° respectively, making those residues almost coplanar.

Magnetic measurements show both salts of [FeL_2]$^{2+}$ are fully high-spin between 5-300 K, as expected from the crystallographic analyses (Figure S11). The complex is also high-spin in CD_3CN solution within the solvent liquid range (Figure S12).[28] That contrasts with the closely related [Fe(tpp)$_2$][BF_4]$_2$ (tpp = 2,4,6-tri(pyrazol-1-yl)pyridine), which shows the clear onset of spin-crossover over the same temperature range with $T_{½}$ = 215 ±3 K.[6] The published correlation between $T_{½}$ and ligand substitutent Hammett parameters in [Fe(bpp)$_2$]$^{2+}$ derivatives cannot be applied here,[6] because the relevant σ_P^+ parameters for *N*-heterocycle substitutents are not available.[29] However the greater π-donor character of an imidazol-1-yl substituent compared to a pyrazol-1-yl group,[30] should destabilize the low-spin form of [FeL_2]$^{2+}$ by reducing Fe→*L* back-bonding and thus lower $T_{½}$, as observed.[6]

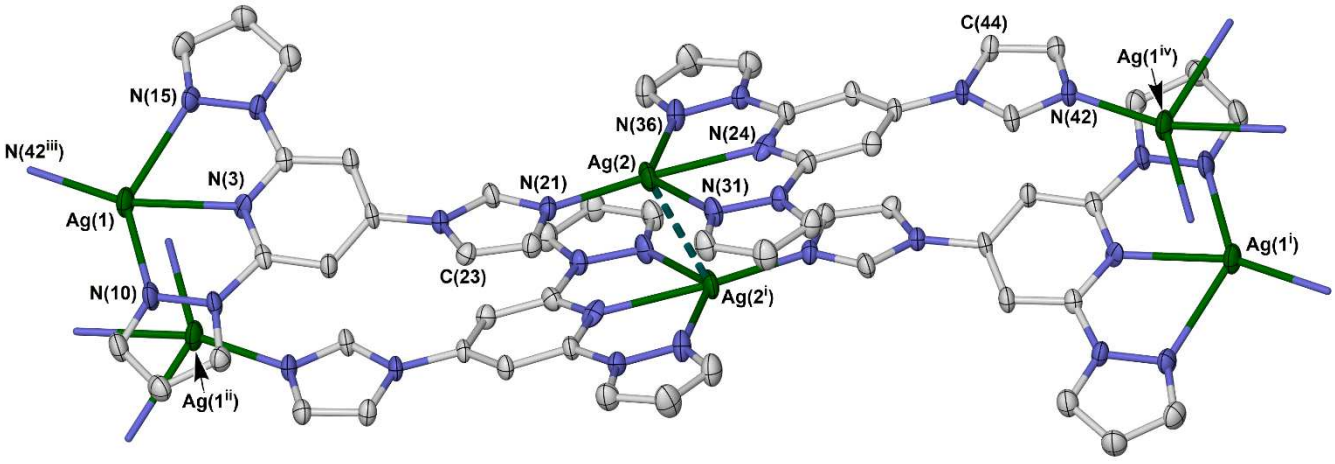

Figure 1 The centrosymmetric dimer-of-1D chains in the coordination polymer [Ag(μ-*L*)]BF_4·½MeCN. Displacement ellipsoids are at the 50 % probability level and the anions, lattice solvent and all H atoms are omitted for clarity. Color code: C, white; Ag, green;N, blue. Symmetry codes: (i) 1−*x*, 1−*y*, 1−*z*; (ii) −*x*, 2−*y*, −*z*; (iii) −1+*x*, 1+*y*, −1+*z*; (iv) 1+*x*, −1+*y*, 1+*z*.

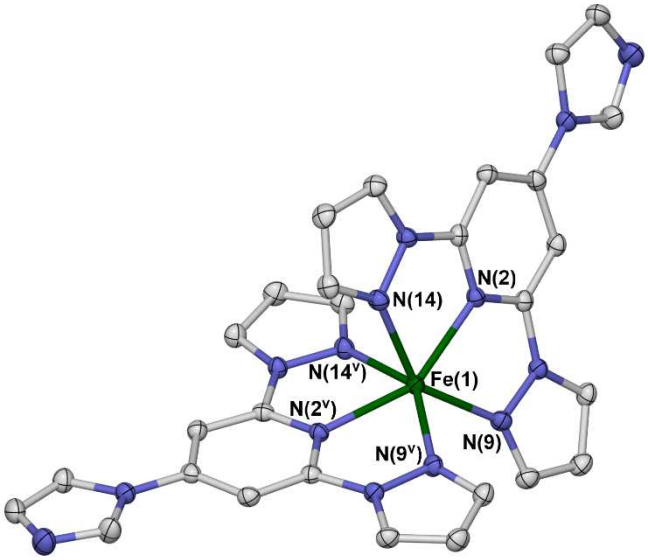

Figure 2 The complex cation in $[FeL_2][BF_4]_2$. Displacement ellipsoids are at the 50 % probability level, and H atoms are omitted for clarity (Figure S##). Color code: C, white; Fe, green; N, blue. Symmetry code: (v) −*x*, *y*, 3/2−*z*.

The ^{1}H NMR spectrum of $[FeL_2][ClO_4]_2$ contains peaks from at least three distinct species (Figure S13). First, contact-shifted peaks at 42.1 (relative integral 8H), 60.7 (4H) and 71.7 (4H) correspond to the four unique protons of the tridentate ligand domain of high-spin $[FeL_2]^{2+}$.[26,31] Second, a collection of peaks between 6.5-9.0 ppm has too large an integral to arise simply from the pendant imidazolyl group of $[FeL_2]^{2+}$, and implies the presence of metal-free *L*. Lastly are additional broad peaks at 11.0 and 14.7 ppm, of 10-12H combined relative integral. These are tentatively ascribed to the uncoordinated bpp residue of a monodentate *L* ligand, although more downfield-shifted peaks from a coordinated imidazolyl ring were not unambiguously identified.[28]

Attempts to form heterometallic assemblies by treating $[FeL_2][BF_4]_2$ or $[FeL_2][ClO_4]_2$ with the appropriate silver salt were unsuccessful, and instead afforded white precipitates of [Ag*L*]X (X^- = BF_4^- or ClO_4^-). This will reflect the lability of high-spin $[FeL_2]^{2+}$ as observed by NMR, and the insolubility of the silver coordination polymers which sequester *L* from these solutions by precipitation.

The bright yellow crystals of $[FeL_2][BF_4]_2$ were sometimes contaminated by a pale green byproduct, which was identified crystallographically as an unusual iron(III)/fluoro species $[Fe_3(\mu\text{-}F)_2F_6L_8]BF_4$ (Fgure 3). The fluoro ligands presumably originate from hydrolysis of BF_4^- during the slow crystallization process, which might be promoted by the basic imidazolyl ligand substituents.[32] This contamination was also evident in the X-ray powder pattern of $[FeL_2][BF_4]_2$; in contrast, samples of $[FeL_2][ClO_4]_2$ were visually homogeneous and phase-pure by powder diffraction (Figure S14).

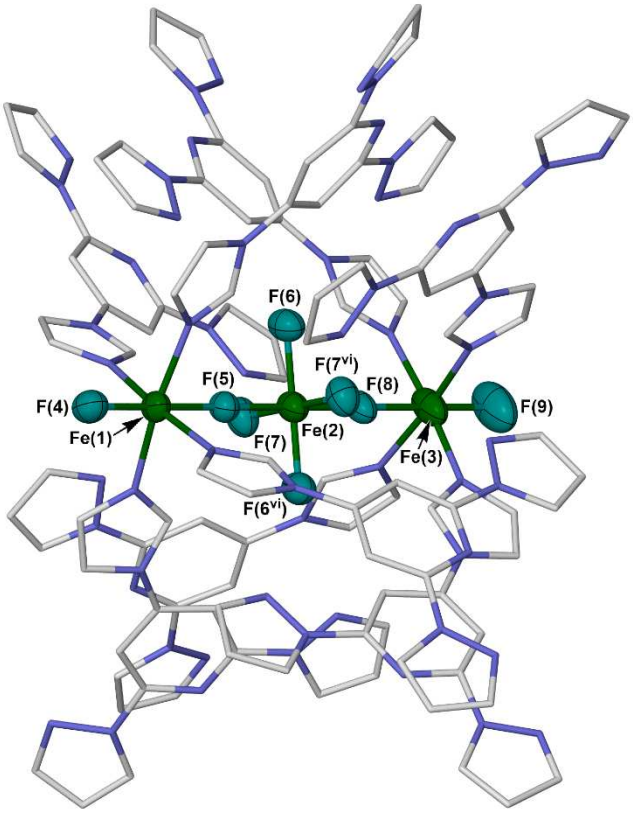

Figure 3 The complex cation in $[Fe_3(\mu\text{-}F)_2F_6L_8]BF_4{\cdot}2.5MeOH$. Only one orientation of the disordered *L* ligand residues is shown, and H atoms are omitted. Fe and F atoms are displayed with 50 % displacement ellipsoids, while the *L* ligands are de-emphasized for clarity (Figure S##). Color code: C, white; F, cyan; Fe, green; N, blue. Symmetry code: (vi) *x*, 1+*x*–*y*, 7/6–*z*.

The identity of the monoatomic ligands in $[Fe_3(\mu\text{-}F)_2F_6L_8]BF_4$ as fluoro rather than (hydr)oxo was confirmed by its mass spectrum. This showed clear molecular ions for $[Fe_3F_8L_8]^+$ (*m*/*z* = 2537.6521; calcd 2537.6552) and $[Fe_3F_7L_8]^{2+}$ (*m*/*z* = 1259.3278; calcd 1259.3281), with few significant fragmentation peaks (Figure S15). These data also confirm the identity of the central hexafluorometallate fragment as $[FeF_6]^{3-}$.[33]

A rational synthesis of $[Fe_3(\mu\text{-}F)_2F_6L_8]BF_4$ was achieved by reaction of $Na_3[FeF_6]$, $Fe[BF_4]_2{\cdot}6H_2O$ and *L* in a 1:2:8 mole ratio in methanol solution. Two pseudopolymorphs of the complex were isolated under different crystallization conditions. Slow evaporation of the reaction mixture yielded large, well-formed cubic crystals (tetragonal, $P4_322$, Z = 8) while slow diffusion of diethyl ether vapor into the methanol solution instead yielded needle-shaped crystals (hexagonal, $P6_122$, Z = 6). Both forms contain 11-13 % solvent-accessible void space, and suffer from mild twinning. A reasonably precise refinement was eventually achieved from a single crystal of the hexagonal form.

The hexagonal crystals have the approximate formula $[Fe_3(\mu\text{-}F)_2F_6L_8]BF_4{\cdot}2.5MeOH$, with the lattice solvent content assigned from a *SQUEEZE* analysis.[34] Their asymmetric unit contains half

a molecule of the complex with the central, linear F(4)−Fe(1)−F(5)−Fe(2)−F(8)−Fe(3)−F(9) spine lying on a crystallographic C_2 axis (Figure 3). Each terminal iron atom is coordinated by four monodentate *L* ligands *via* their imidazolyl N-donors, while the central Fe atom is bound by four terminal fluoride ions. Hence, an alternative formulation of the molecule is $[\{trans\text{-}Fe^{III}FL_4\}_2(\mu\text{-}F)_2Fe^{III}F_4]^+$. The +3 oxidation states of all three iron atoms were supported by a bond-valence sum (BVS) calculation,[35] which yielded BVS values of 2.783(12), 3.209(9) and 2.82(2) for Fe(1)-Fe(3) respectively. The bridging Fe−(μ-F) bond lengths [1.949(4)-1.986(4) Å] are in the usual range for $[FeF_6]^{3-}$-containing species (Table S4).[33,36,37] The terminal Fe−F distances [1.847(4)-1.887(5) Å] are shorter, but also have precedent in iron(III) fluoro complexes.[33,38] The Fe−N bonds lie between 2.111(7)-2.128(5) Å.

While there are no hydrogen bond donors in the molecule, each *L* ligand forms two chelating C−H...F contacts to F(6), F(7) or their symmetry equivalents (Figures 4 and S17, Table S5). The shortest interactions involve the imidazolyl *C*2 C−H groups [C...F = 3.053(10)-3.075(11) Å] with a second, longer contact also formed by the pyridyl *C*3 C−H groups [C...F = 3.315(10)-3.350(9) Å]. These interactions encapsulate the $[FeF_6]^{3-}$ moiety within a hydrophobic cavity at the centre of the molecule, which may contribute to the stability of the assembly in solution (see above). The short contacts to the metal-coordinated imidazolyl C−H groups are comparable to the C−H...X^- distances formed by imidazolium anion host molecules.[39]

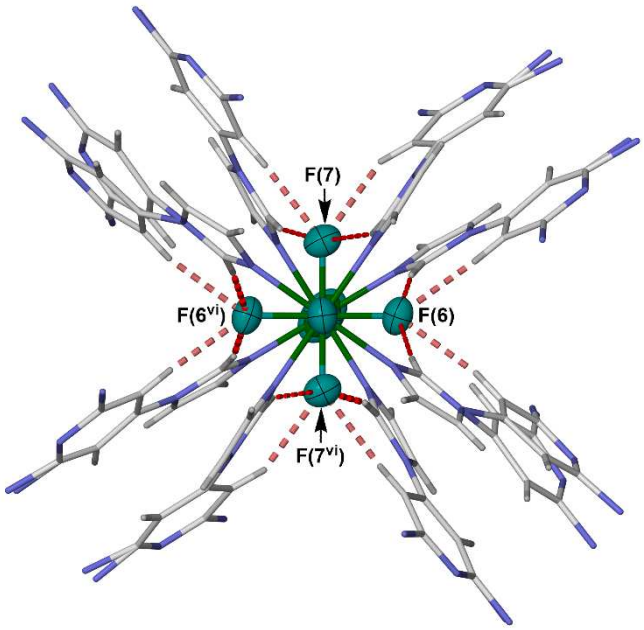

Figure 4 View of the $[Fe_3(\mu\text{-}F)_2F_6L_8]^+$ cation down its C_2 symmetry axis, showing the short (dark red) and long (pale red) C−H...F interactions to the $[FeF_6]^{3-}$ moiety. Both orientations of disordered ligand residues, and H atoms, are included but only the *ipso* N atoms of the peripheral pyrazolyl groups are shown. Other details as for Figure 3. One pyridyl group interacting with F(6) and F(6vi) is disordered, with only one disorder site forming a C−H...F contact.

It proved challenging to obtain $[Fe_3(\mu\text{-}F)_2F_6L_8]BF_4$ free from contamination by $[FeL_2][BF_4]_2$. Small quantities of the pure compound were ultimately produced by lightly sonicating the crystallization vials, then decanting off microcrystalline contaminants. The sonication destroyed the needle-shaped hexagonal crystals as well as the impurities, but allowed the more robust cubic tetragonal crystals to be separated from the mixture. The resultant polycrystalline materials were analytically pure but poorly crystalline by powder diffraction (Figure S21), which could reflect damage during the sonication process.

A sample of the cubic crystals showed $\chi_M T$ = 6.2 $cm^3mol^{-1}K$ at 300 K, which is below the predicted value of *ca* 13 $cm^3mol^{-1}K$ for three independent S = 5/2 iron(III) centers. Cooling the sample leads to an almost monotonic reduction in $\chi_M T$, which reaches 3.8 $cm^3mol^{-1}K$ at 40 K before decreasing more quickly below that temperature (Figure 5). The latter decrease is attributed to zero-field splitting effects, which are expected to be weak but non-zero.[40] Intermolecular coupling interactions can also influence $\chi_M T$ at low temperatures but are unlikely to be significant in this case, because the magnetic $[Fe_3F_8]^+$ centers in the material are well-separated from each other by the peripheral *L* ligands.

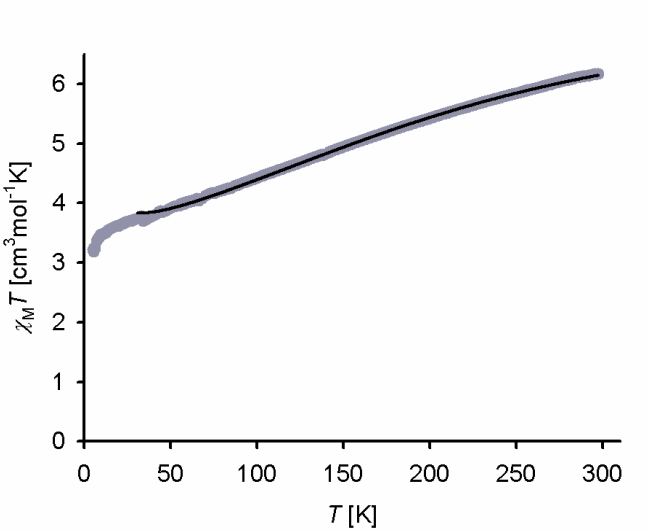

Figure 5 Variable temperature magnetic susceptibility data for $[Fe_3(\mu\text{-}F)_2F_6L_8]BF_4$. The black line shows the best fit of the data to the van Vleck equation derived from eq 1.[41]

The data were modelled by the following Hamiltonian (eq 1):

$$\hat{H} = -2J_1(S_1 \cdot S_2 + S_2 \cdot S_3) - 2J_2(S_1 \cdot S_3) \qquad (1)$$

where S_1-S_3 are the S = 5/2 spins of the corresponding iron atoms in the crystal structure, Fe(1)-Fe(3) (Figure 3). In this formalism, J_1 represents the coupling between iron atoms bridged by fluoride ligands, while J_2 is a weaker interaction between the terminal iron centers. The van Vleck equation derived from this Hamiltonian[41] reproduced the data above 30 K very well, with the refined parameters J_1 = −29.1(2) cm^{-1}, J_2 = −6.3(7) cm^{-1} and g = 2.001(2) (R^2 = 0.999, Figure 5). This pattern of J couplings corresponds to

an S = 5/2 magnetic ground state for the molecule, lying 82 cm^{-1} below a S = 3/2 first excited spin state.

The additional decrease in $\chi_M T$ below 30 K could also be fit by the model, but this requires a higher g value of *ca* 2.15 which is not physically realistic for S = 5/2 iron(III) (Figures S22 and S23).[42] That supports the involvement of zero-field splitting in the low-temperature data. Alternative fits with J_2 fixed at 0 were also clearly inferior to the one in Figure 5 (Figure S24). We propose the multiple C−H...F interactions involving the *L* ligands might provide a superexchange pathway between Fe(1) and Fe(3), giving rise to the unexpectedly large J_2 value.

To our knowledge, there is one previous magnetochemical study of molecular $Fe^{III}_2(\mu\text{-F})$ complexes with (approximately) linear fluoride bridging ligands. These are salts of $[Fe_2(\mu\text{-F})L]^+$, where H_4L is one of two cofacial *bis*(octaethylporphyrin) derivatives. The antiferromagnetic coupling constants in those compounds, $-33 \geq J \geq -39$ cm^{-1}, are in good agreement with J_1 from this analysis.[43]

Conclusions

The new ditopic bpp derivative *L* has been synthesized in two steps from commercially available precursors, in 40 % overall yield.[5] The tridentate and monodentate binding sites of *L* can coordinate metal ions individually or simultaneously, based on the compounds in this work. *L* proved unsuitable for the synthesis of spin-crossover iron/silver materials[16] because the electronic influence of the imidazol-1-yl substituent enforces a labile high-spin state on $[FeL_2]^{2+}$; and, because $[FeL_2]^{2+}$ proved unexpectedly labile in solution by ^{1}H NMR (Figure S13). That facilitates precipitation of insoluble $[Ag(\mu\text{-}L)]^+$ salts upon addition of silver reagents to $[FeL_2]^{2+}$, thus precluding the formation of mixed-metal assemblies. Significant ligand displacement is not often observed in ^{1}H NMR spectra of high-spin $[Fe(bpp)_2]^{2+}$ derivatives.[30] We propose the nucleophilic imidazolyl group in *L* competes with the tridentate ligand domain for metal binding, leading to the mixture of solution species observed. However, assembly of more robust $[ML_2]^{2+}$ centers (*eg* M = Ru) with silver salts or other linkers could be a promising route to heterometallic gels or other assembly structures.

$[Fe_3(\mu\text{-F})_2F_6L_8]^+$ is a rare example of a metal/organic fluoro-bridged iron complex with an all-iron(III) oxidation level.[43-46] The μ-$[MF_6]^{n-}$ (M = a transition metal) bridging ligand motif is also rarely seen in molecular complexes,[47,48] although coordination polymers containing hexafluorometallate linkers are better known.[36,49] In principle, a range of multimetallic $[\{ML_4\}_2(\mu\text{-}F)_2M'F_4]^{n+}$ species containing different metal ions could be accessed, by reacting *L* with the appropriate $Na_3[M'F_6]$ and $M[BF_4]_2$ precursors. This is currently under investigation.

Experimental Section

Instrumentation

Elemental microanalyses were performed by the microanalytical services at the University of Leeds School of Chemistry, and the London Metropolitan University School of Human Sciences. Electrospray mass spectra (ESMS) were obtained on a Bruker MicroTOF spectrometer, from MeCN feed solutions. All mass peaks have the correct isotopic distributions for the proposed assignments. NMR spectra were obtained using a Bruker Avance 500 FT spectrometer operating at 500.1 MHz (^{1}H) or 125 MHz (^{13}C). Magnetic susceptibility measurements in solution were obtained by Evans method using a Jeol JNM-ECA600II (600.1 MHz) spectrometer.[50] Tetramethylsilane was added to all the solutions as an internal standard. A diamagnetic correction for the sample,[51] and a correction for the variation of the density of the solvent with temperature,[52] were applied to these data. Processing and curve fitting of magnetic data was performed using *SIGMAPLOT*.[53]

Solid state magnetic susceptibility measurements were performed with freshly isolated, unground polycrystalline samples, using a Quantum Design MPMS-3 magnetometer in an applied field of 5000 G and a temperature ramp of 5 $Kmin^{-1}$. Diamagnetic corrections for the samples were estimated from Pascal's constants;[51] a previously measured diamagnetic correction for the sample holder was also applied to the data. Solvated samples were protected against solvent loss by saturating the (tightly sealed) sample holder capsules with a drop of diethyl ether. X-ray powder diffraction measurements were obtained from a Bruker D2 Phaser diffractometer, using Cu K_α radiation (λ = 1.5418 Å).

Materials and methods

Unless otherwise stated, all reactions were carried out in air using as-supplied AR-grade solvents. All reagents and solvents were purchased commercially and used as supplied.

Synthesis of 2,6-difluoro-4-(imidazol-1-yl)-pyridine. Imidazole (1.00 g, 14.7 mmol) was carefully added to a suspension of sodium hydride (60 wt % in mineral oil; 0.70 g, 17 mmol) in tetrahydrofuran (35 cm^3) under a nitrogen atmosphere. After evolution of hydrogen had ceased, excess 2,4,6-trifluoropyridine (5.00 g, 38 mmol) was added and the mixture was stirred at room temperature for 5 hrs. After evaporation to dryness and extraction with dichloromethane, colorless needles of the product were isolated from the mixture following silica flash column chromatography (Rf 0.52, ethyl acetate eluent). Yield 1.29 g, 48 %. Mp 164-165 °C. ESMS *m/z* 182.0530 (calcd for $[(C_8H_5F_2N_3)H]^+$ 182.0524). ^{1}H NMR ({CD_3}$_2$SO) δ 7.20 (d, 0.7 Hz, 1H, Im H^5), 7.72 (m, 2H, Py $H^{3/5}$), 8.06 (d, 0.7 Hz, 1H, Im H^4), 8.64 (s, 1H, Im H^2). ^{13}C NMR ({CD_3}$_2$SO) δ 97.3 (m, 2C, Py $C^{3/5}$), 118.1 (1C, Im C^4), 131.5 (1C, Im C^5), 136.8 (1C, Im C^2), 151..4 (t, 14 Hz, 1C, Py C^4), 162.5 (dd, 23 and 298 Hz, 2C, Py $C^{2/6}$).

Synthesis of 4-(imidazol-1-yl)-2,6-di(pyrazol-1-yl)pyridine (*L*). Pyrazole (0.60 g, 8.8 mmol) was carefully added to a suspension of sodium hydride (60 wt % in mineral oil; 0.36 g, 8.8 mmol) in tetrahydrofuran (15 cm^3) under a nitrogen atmosphere. After evolution of hydrogen had ceased, 2,6-di(fluoro)-4-(imidazol-1-yl)-pyridine (0.76 g, 4.2 mmol) was added to the mixture. The solution was stirred at room temperature for 24 hrs. After evaporation to dryness and extraction of the residue with dichloromethane, silica flash column chromatography yielded the product as a white powder (Rf 0.33, ethyl acetate eluent). Yield 0.98 g, 84 %. Mp 196-197 °C. ESMS *m/z* 278.1157 (100 %; calcd for $[HL]^+$ 278.1154), 300.0973 (48 %; calcd for $[NaL]^+$ 300.0974). ^{1}H NMR ($CDCl_3$) δ 6.42 (pseudo-t, 2.7 Hz, 2H, Pz H^4), 7.18 (s, 1H, Im H^5), 7.44 (s, 1H, Im H^4), 7.68 (d, 2.5 Hz, 2H, Pz H^3), 7.77 (s, 2H, Py $H^{3/5}$), 8.10 (s, 1H, Im H^2), 8.44 (d, 2.7 Hz, 2H, Pz H^5); ^{13}C NMR ($CDCl_3$) δ 99.5 (2C, Py $C^{3/5}$), 108.6 (2C, Pz C^4), 117.0 (1C, Im C^4), 127.4 (2C, Pz C^5), 131.7 (1C, Im C^5), 135.2 (1C, Im C^2), 143.1 (2C, Pz C^3),

147.9 (1C, Py C^4), 151.6 (2C, Py $C^{2/6}$); elemental analysis calcd (%) for $C_{14}H_{11}N_7$ (277.29): C 60.6, H 4.00, N 35.4; found: C 60.2, H 4.00, N 35.6.

Synthesis of *catena*-[Ag(*μ*-*L*)]BF_4. A solution of *L* (19 mg, 0.068 mmol) in acetonitrile (2.5 cm^3) was added to a solution of $AgBF_4$ (13 mg, 0.068 mmol) in the same solvent (8 cm^3). The solution was left to evaporate very slowly in a sealed vial, which afforded colorless single crystals of [Ag*L*]BF_4·½MeCN after three months. Exposing these crystals to air leads to replacement of the acetonitrile solvent by atmospheric moisture, affording a white material analysing approximately as [Ag*L*]BF_4·½H_2O. Yield 15 mg, 47 %. ESMS *m/z* 278.1169 (11 %; calcd for $[HL]^+$ 278.1154), 384.0875 (100 %; calcd for $[AgL]^+$ 384.0121), 425.0838 (36 %; calcd for $[AgL(NCCH_3)]^+$ 425.0387), 661.2443 (23 %; calcd for $[AgL_2]^+$ 661.1197); elemental analysis calcd (%) for $C_{14}H_{11}AgBF_4N_7$·½H_2O (480.97): C 35.0, H 2.51, N 20.4; found: C 34.5, H 2.41, N 20.8.

Synthesis of [Fe*L*$_2$][BF_4]$_2$. Solutions of *L* (10 mg, 0.036 mmol) in acetonitrile (3 cm^3) and of $Fe[BF_4]_2$·6H_2O (6 mg, 0.018 mmol) in acetonitrile (1 cm^3) were mixed, leading to an immediate bright yellow coloration. Addition of excess diethyl ether afforded a yellow precipitate, which was collected by filtration. Recrystallization of the powder by slow diffusion of diethyl ether vapor into an acetonitrile solution of the powder yielded bright yellow single crystals of the complex. Yield 11 mg, 82 %. ESMS *m/z* 278.1714 (100 %; calcd for $[HL]^+$ 278.1154), 305.1351 (61 %; calcd for $[FeL_2]^{2+}$ 305.0751), 352.1946 (16 %; calcd for $[FeLF]^+$ 352.1322), 629.2715 (9 %; calcd for $[FeL_2F]^+$ 629.1485); elemental analysis calcd (%) for $C_{28}H_{22}B_2F_8FeN_{14}$ (784.03): C 42.9, H 2.83, N 25.0; found: C 43.0, H 2.92, N 24.8.

Synthesis of [Fe*L*$_2$][ClO_4]$_2$. Method as for [FeL_2][BF_4]$_2$, using $Fe[ClO_4]_2$·6H_2O (7 mg, 0.018 mmol). The product formed yellow single crystals from acetonitrile/diethyl ether. Yield 10 mg, 71 %; elemental analysis calcd (%) for $C_{28}H_{22}Cl_2FeN_{14}O_8$ (809.32): C 41.6, H 2.74, N 24.2; found: C 41.7, H 2.62, N 24.1. The ^1H NMR spectrum of this complex is discussed in the Supporting Information (Figure S13).

Synthesis of [Fe_3(*μ*-F)$_2$$F_6$(*L*)$_8$]$BF_4$. A solution of *L* (35 mg, 0.13 mmol) in methanol (4 cm^3) was mixed with a suspension of $Na_3[FeF_6]$ (3.8 mg, 0.016 mmol) in the same solvent (2 cm^3). Addition of a third solution of $Fe[BF_4]_2$·6H_2O (11 mg, 0.032 mmol) in methanol (3 cm^3) led to formation of a pale green/yellow color. Slow evaporation of the filtered solution yielded large cubic crystals of the product, which suffered from twinning and were consistently contaminated with [FeL_2][BF_4]$_2$ by powder diffraction. Alternatively, slow diffusion of diethyl ether vapor into the same reaction mixture gave a lower yield of needle-shaped crystals, which were sometimes suitable for crystallographic analysis. Light sonication of the crystallization vials and removal of the microcrystalline impurities by decantation, afforded the product in analytical purity. Yield 18 mg, 44 %. ESMS *m/z* 1249.8282 (25 %; calcd for $[Fe_3F_6L_8]^{2+}$ 1249.8291), 1259.3278 (100 %; calcd for $[Fe_3F_7L_8]^{2+}$ 1259.3281), 2537.6521 (6 %; calcd for $[Fe_3F_8L_8]^+$ 2537.6552); elemental analysis calcd (%) for $C_{112}H_{88}BF_{12}Fe_3N_{56}$ (2624.63): C 51.3, H 3.38, N 29.9; found: C 51.2, H 3.32, N 29.8.

Single-crystal structure analyses

Crystals of *L* were obtained from $CDCl_3$ solution; the crystallization procedures for the other compounds are described above. All diffraction data were collected with an Agilent Supernova dual source diffractometer using monochromated Cu-K_α radiation (λ = 1.54184 Å). Experimental details of the structure determination of each compound and full details of all the crystallographic refinements, are given in the Supporting Information (Table S1). The structures were solved by direct methods (*SHELXS97*),[54] and developed by full least-squares refinement on F^2 (*SHELXL97*).[54] Crystallographic figures were prepared using *X-SEED*,[55] while *OLEX2* was used for calculations of structural parameters.[56] Bond-valence sum calculations employed literature parameters for high-spin Fe –N and Fe–F bonds.[57]

CCDC 1997941 (for 2,6-difluoro-4-(imidazol-1-yl)-pyridine), 1997942 (for *α*-*L*), 1997943 (for [Ag(*μ*-*L*)]BF_4·½CH_3CN), 1997944 (for [FeL_2][BF_4]$_2$), 1997945 (for [FeL_2][ClO_4]$_2$), and 1997946 (for [Fe_3(*μ*-F)$_2$$F_6$$L_8$]$BF_4$·2.5$CH_3OH$) contain the supplementary crystallographic data for this paper. These data can be obtained free of charge from The Cambridge Crystallographic Data Centre.

Acknowledgements

This work was funded by the Leverhulme Trust (RPG-2015-095) and the EPSRC (EP/K012576/1). The authors thank Dr Mark Howard (School of Chemistry, University of Leeds) for the Evans method measurement.

Keywords: iron • silver • N-donor ligands • X-ray crystallography • magnetic measurements

[1] The 1-bpp nomenclature is sometimes used to distinguish 2,6-di(pyrazol-1-yl)pyridines from the regioisomeric 2,6-di(1*H*-pyrazol-3-yl)pyridine.(3-bpp) derivatives, which are also popular ligands for spin-crossover compounds, supramolecular chemistry and catalysis.[25]

[2] a) M. A. Halcrow, *Coord. Chem. Rev.* **2005**, *249*, 2880–2908; b) M. A. Halcrow, *New J. Chem.* **2014**, *38*, 1868–1882.

[3] a) M. A. Halcrow, *Coord. Chem. Rev.* **2009**, *253*, 2493–2514; b) L. J. Kershaw Cook, R. Mohammed, G. Sherborne, T. D. Roberts, S. Alvarez, M. A. Halcrow, *Coord. Chem. Rev.* **2015**, *289–290*, 2–12.

[4] J. Olguin, S. Brooker, *Coord. Chem. Rev.* **2011**, *255*, 203–240.

[5] M. Attwood, S. S. Turner, *Coord. Chem. Rev.* **2017**, *353*, 247–277.

[6] L. J. Kershaw Cook, R. Kulmaczewski, R. Mohammed, S. Dudley, S. A. Barrett, M. A. Little, R. J. Deeth, M. A. Halcrow, *Angew. Chem. Int. Ed.* **2016**, *55*, 4327–4331; *Angew. Chem.* **2016**, *128*, 4399–4403.

[7] M. A. Halcrow, I. Capel Berdiell, C. M. Pask, R. Kulmaczewski, *Inorg. Chem.* **2019**, *58*, 9811−9821.

[8] a) L. J. Kershaw Cook, F. L. Thorp-Greenwood, T. P. Comyn, O. Cespedes, G. Chastanet, M. A. Halcrow, *Inorg. Chem.* **2015**, *54*, 6319−6330; b) K. S. Kumar, B. Heinrich, S. Vela, E. Moreno-Pineda, C. Bailly, M. Ruben, *Dalton Trans.* **2019**, *48*, 3825−3830.

[9] See *eg* a) M. Nihei, N. Takahashi, H. Nishikawa, H. Oshio, *Dalton Trans.* **2011**, *40*, 2154–2156; b) K. Takahashi, Y. Hasegawa, R. Sakamoto, M. Nishikawa, S. Kume, E. Nishibori, H. Nishihara, *Inorg. Chem.* **2012**, *51*, 5188–5198; c) A. Santoro, L. J. Kershaw Cook, R. Kulmaczewski, S. A. Barrett, O. Cespedes, M. A. Halcrow, *Inorg. Chem.* **2015**, *54*, 682–693; d) A. Abhervé, M. Palacios-Corella, J. M. Clemente-Juan, R. Marx, P. Neugebauer, J. van Slageren, M. Clemente-León, E. Coronado, *J. Mater. Chem. C* **2015**, *3*, 7936–7945; e) A. Abhervé, M. J. Recio-Carretero, M. López-Jordà, J. M. Clemente-Juan, J. Canet-Ferrer, A. Cantarero, M. Clemente-León, E. Coronado, *Inorg. Chem.* **2016**, *55*, 9361–9367; f) B. Schäfer, T. Bauer, I. Faus, J. A. Wolny, F. Dahms, O. Fuhr, S. Lebedkin, H.-C. Wille, K. Schlage, K. Chevalier, F. Rupp, R. Diller, V. Schünemann, M. M. Kappes, M. Ruben, *Dalton Trans.* **2017**, *46*, 2289–2302.

[10] See *eg* a) M. S. Alam, M. Stocker, K. Gieb, P. Müller, M. Haryono,K. Student, A. Grohmann, *Angew. Chem. Int. Ed.* **2010**, *49*, 1159–1163; *Angew. Chem.* **2010**, *122*, 1178–1182; b) V. Meded, A. Bagrets, K. Fink,

R. Chandrasekar, M. Ruben, F. Evers, A. Bernand-Mantel, J. S. Seldenthuis, A. Beukman, H. S. J. van der Zant, *Phys. Rev. B* **2011**, ***83***, 245415; c) E. J. Devid, P. N. Martinho, M. V. Kamalakar, I. Šalitroš, U. Prendergast, J.-F. Dayen, V. Meded, T. Lemma, R. González-Prieto, F. Evers, T. E. Keyes, M. Ruben, B. Doudin, S. J. van der Molen, *ACS Nano* **2015**, *9*, 4496–4507; d) K. S. Kumar, I. Šalitroš, Z. Boubegtiten-Fezoua, S. Moldovan, P. Hellwig, M. Ruben, *Dalton Trans.* **2018**, *47*, 35–40; e) E. Burzurí, A. García-Fuente, V. García-Suárez, K. S. Kumar, M. Ruben, J. Ferrer, H. S. J. van der Zant, *Nanoscale* **2018**, *10*, 7905–7911.

[11] See *eg* a) M. Starck, P. Kadjane, E. Bois, B. Darbouret, A. Incamps, R. Ziessel, L. J. Charbonnière, *Chem. Eur. J.* **2011**, *17*, 9164–9179; b) M. Starck, R. Ziessel, *Dalton Trans.* **2012**, *41*, 13298–13307; c) M. Feng, F. Pointillart, B. Le Guennic, B. Lefeuvre, S. Golhen, O. Cador, O. Maury, L. Ouahab, *Chem. Asian J.* **2014**, *9*, 2814–2825; d) Y. S. L. V. Narayana, M. Baumgarten, K. Müllen, R. Chandrasekar, *Macromolecules* **2015**, *48*, 4801−4812; e) D. J. Strohecker, V. M. Lynch, B. J. Holliday, R. A. Jones, *Dalton Trans.* **2017**, *46*, 7733–7742.

[12] a) K. M. Arendt, A. G. Doyle, *Angew. Chem. Int. Ed.* **2015**, *54*, 9876–9880; *Angew. Chem.* **2015**, *127*, 10014–10018; b) B. P. Woods, M. Orlandi, C.-Y. Huang, M. S. Sigman, A. G. Doyle, *J. Am. Chem. Soc.* **2017**, *139*, 5688–5691; c) C. Heinz, J. P. Lutz, E. M. Simmons, M. M. Miller, W. R. Ewing, A. G. Doyle, *J. Am. Chem. Soc.* **2018**, *140*, 2292–2300.

[13] a) S. W. Smith, G. C. Fu, *Angew. Chem. Int. Ed.* **2008**, *47*, 9334 –9336; *Angew. Chem.* **2008**, *120*, 9474-9476; b) S. Plunkett, C. H. Basch, S. O. Santana, M. P. Watson, *J. Am. Chem. Soc.* **2019**, *141*, 2257−2262.

[14] See *eg* a) Y.-T. Li, B.-S. Liao, H.-P. Chen, S.-T. Liu, *Synthesis* **2011**, 2639−2643; b) W. Du, Q. Wang, L. Wang, Z. Yu, *Organometallics* **2014**, *33*, 974−982; c) D. Gong, X. Jia, B. Wang, X. Zhang, K.-W. Huang, *J. Organomet. Chem.* **2014**, *766*, 794−85; d) M. N. Magubane, G. S. Nyamato, S. O. Ojwach, O. Q. Munro, *RSC Adv.* **2016**, *6*, 65205−65221; e) Z. Cao, H. Qiao, F. Zeng, *Organometallics* **2019**, *38*, 797−804.

[15] a) J. Burschka, F. Kessler, M. K. Nazeeruddin, M. Grätzel, *Chem. Mater.* **2013**, *25*, 2986−2990; b) S. P. Hill, K. Hanson, *J. Am. Chem. Soc.* **2017**, *139*, 10988−10991.

[16] I. Capel Berdiell, A. N. Kulak, S. L. Warriner, M. A. Halcrow, *ACS Omega* **2018**, *3*, 18466−18474.

[17] I. Capel Berdiell, S. L. Warriner, M. A. Halcrow, *Dalton Trans.* **2018**, *47*, 5269–5278.

[18] I. Capel Berdiell, S. E. Farmiloe, R. Kulmaczewski, M. A. Halcrow, *Dalton Trans.* **2019**, *48*, 17310–17320.

[19] I. Capel Berdiell, T. Hochdörffer, C. Desplanches, R. Kulmaczewski, N. Shahid, J. A. Wolny, S. L. Warriner, O. Cespedes, V. Schünemann, G. Chastanet, M. A. Halcrow, *J. Am. Chem. Soc.* **2019**, *141*, 18759–18770.

[20] a) M. Schlosser, T. Rausis, C. Bobbio, *Org. Lett.* **2005**, *7*, 127–129; b) M. Schlosser, C. Bobbio, T. Rausis, *J. Org. Chem.* **2005**, *70*, 2494–2502.

[21] K. M. Steed, J. W. Steed, *Chem. Rev.* **2015**, *115*, 2895–2933.

[22] A. G. Young, L. R. Hanton, *Coord. Chem. Rev.* **2008**, *252*, 1346–1386.

[23] H. Schmidbaur, A. Schier, *Angew. Chem. Int. Ed.* **2015**, *54*, 746–784; *Angew. Chem.* **2015**, *127*, 756–797.

[24] See *eg* a) M. J. Hannon, C. L. Painting, E. A. Plummer, L. J. Childs, N. W. Alcock, *Chem. Eur. J.* **2002**, *8*, 2226–2238; b) R. Zibaseresht, R. M. Hartshorn, *Dalton Trans.* **2005**, 3898--3908; c) M. C. Carrión, I. M. Ortiz, F. A. Jalón, B. R. Manzano, A. M. Rodríguez, J. Elguero, *Cryst. Growth Des.* **2011**, *11*, 1766–1776; d) G. M. Borrajo-Calleja, E. de Julián, E. Bayón, J. Díez, E. Lastra, I. Merino, M. P. Gamasa, *Inorg. Chem.* **2016**, *55*, 8794–8807.

[25] G. A. Craig, O. Roubeau, G. Aromí, *Coord. Chem. Rev.* **2014**, *269*, 13–31.

[26] J. M. Holland, J. A. McAllister, C. A. Kilner, M. Thornton-Pett, A. J. Bridgeman, M. A. Halcrow, *J. Chem. Soc. Dalton Trans.* **2002**, 548–554.

[27] S. Vela, J. J. Novoa, J. Ribas-Arino, *Phys. Chem. Chem. Phys.* **2014**, *16*, 27012–27024.

[28] The ligand displacement processes detected by ^{1}H NMR would not prevent the observation of SCO for $[FeL_2]^{2+}$ in solution, if this occurred within the liquid range of the solvent. See *eg* a) N. Hassan, A. B. Koudriavtsev, W. Linert, *Pure Appl. Chem.* **2008**, *80*, 1281–1292; b) S. A. Barrett, C. A. Kilner, M. A. Halcrow, *Dalton Trans.* **2011**, *40*, 12021–12024; c) H. Petzold, P. Djomgoue, G. Hörner, C. Lochenie, B. Weber, T. Rüffer, *Dalton Trans.* **2018**, *47*, 491–506.

[29] C. Hansch, A. Leo, R. W. Taft, *Chem. Rev.* **1991**. *97,* 165–195.

[30] C. Curutchet, J. Poater, M. Solà, J. Elguero, *J. Phys. Chem. A* **2011**, *115*, 8571–8577.

[31] J. M. Holland, S. A. Barrett, C. A. Kilner, M. A. Halcrow, *Inorg. Chem. Commun.* **2002**, *5*, 328–332.

[32] J. Reedijk, *Comments Inorg. Chem.* **1982**, *1*, 379–389.

[33] The Fe−F distances to Fe(2) are 0.2 Å too long to be consistent with an alternative potential assignment of the central residue, as a μ-$[SiF_6]^{2-}$ ion (Table S4).

[34] A. L. Spek, *Acta Cryst. Sect. C: Struct. Chem*. **2015**. *71*, 9–18.

[35] M. O'Keeffe, *Struct. Bonding (Berlin)* **1989**, *71*, 161−190.

[36] a) E. Herdtweck, J. Graulich, D. Babel, Z. *Naturforsch. Teil B: Chem. Sci.* **1990**, *45*, 161−169; b) A. B. Ali, J.-M. Grenèche, M. Leblanc, V. Maisonneuve, *Solid State Sci.* **2009**, *11*, 1631–1638; c) G. Darmograi, L. Jouffret, A. Hémon-Ribaud, M. Leblanc, V. Maisonneuve, J. Lhoste, *Z. Anorg. Allg. Chem.* **2014**, *640*, 1385–1391; d) V. Pimenta, J. Lhoste, A. Hémon-Ribaud, M. Leblanc, J.-M. Grenèche, L. Jouffret, A. Martel, G. Dujardin, V. Maisonneuve, *Cryst. Growth Des.* **2015**, *15*, 4248−4255.

[37] a) M. Dan, *J. Mol. Struct.* **2004**, *706*, 127−131; b) S. Bouketaya, M. Smida, M. S. M. Abdelbaky, M. Dammak, S. Garcia-Granda, *J. Solid State Chem.* **2018**, *262*, 343–350.

[38] For iron(III) complexes with terminal fluoro ligands see *eg*: a) S. Christie, S. Subramanian, L. Wang, M. J. Zaworotko, *Inorg. Chem.* **1993**, *32*, 5415–5417; b) R. Leo, W. Massa, J. Pebler, *J. Fluorine Chem.* **2004**, *125*, 923–935; c) L. R. Widger, Y. Jiang, A. C. McQuilken, T. Yang, M. A. Siegler, H. Matsumura, P. Moënne-Loccoz, D. Kumar, S. P. de Visser, D. P. Goldberg, *Dalton Trans.* **2014**, *43*, 7522–7532; d) K. S. Pedersen, G. Lorusso, J. J. Morales, T. Weyhermüller, S. Piligkos, S. K. Singh, M. Schau-Magnussen, G. Rajaraman, M. Evangelisti, J. Bendix, *Angew Chem. Int. Ed.* **2014**, *53*, 2394–2397; *Angew Chem.* **2014**, *126*, 2426–2429; e) K. L. M. Harriman, I. A. Kühne, A. A. Leitch, I. Korobkov, R. Clérac, M. Murugesu, J. L. Brusso, *Inorg. Chem.* **2016**, *55*, 5375–5383; f) T. P. Zimmermann, S. Dammers, A. Stammler, H. Bögge, T.Glaser, *Eur. J. Inorg. Chem.* **2018**, 5229–5237.

[39] See *eg* a) Y. Yuan, G. Gao, Z.-L. Jiang, J.-S. You, Z.-Y. Zhou, D.-Q. Yuan, R.-G. Xie, *Tetrahedron* **2002**, *58*, 8993–8999; b) N. J. Singh, E. J. Jun, K. Chellappan, D. Thangadurai, R. P. Chandran, I.-C. Hwang, J. Yoon, K. S. Kim, *Org. Lett.* **2007**, *9*, 485−488; c) E. Alcalde, N. Mesquida, M. Vilaseca, C. Alvarez-Rúa, S. García-Granda, *Supramol. Chem.* **2007**, *19*, 501–509; d) C. E. Willans, K. M. Anderson, L. C. Potts, J. W. Steed, *Org. Biomol. Chem.* **2009**, *7*, 2756–2760; e) Y. Chun, N. J. Singh, I.-C. Hwang, J. W. Lee, S. U. Yu, K. S Kim, *Nature Commun.* **2013**, *4*, 2758; f) Z. Li, N. Wiratpruk, P. J. Barnard, *Front. Chem.* **2019**, *7*, 270.

[40] R. Boča, *Coord. Chem. Rev.* **2004**, *248*, 757–815.

[41] S. M. Gorun, G. C. Papaefthymiou, R. B. Frankel, S. J. Lippard, *J. Am. Chem. Soc.* **1987**, *109*, 4244–4255.

[42] The parameters from fitting the magnetic data over the full temperature range were J_1 = −35.9(2) cm^{-1}, J_2 = −10.8(7) cm^{-1} and g = 2.142(2) (R^2 = 0.997; Figure S22). While the fit is good these results are not physically reasonable, because g should be close to 2.00 for S = 5/2 iron(III) spins.[40]

[43] Di-iron(III) complexes with a bridging fluoro ligand: D. Sil, A. Kumar, S. P. Rath, *Chem. Eur. J.* **2016**, *22*, 11214–11223.

[44] A tetra-iron(III) complex with bridging fluoro ligands: K. Mason, I. A. Gass, S. Parsons, A. Collins, F. J. White, A. M. Z. Slawin, E. K. Brechin, P. A. Tasker, *Dalton Trans.* **2010**, *39*, 2727–2734.

[45] Mixed-valent iron(II/III) complexes with bridging fluoro ligands: a) H. Sugimoto, Y. Hayashi, C. Koshi, S. Fujinami, M. Suzuki, Y. Maeda, A. Uehara, *Chem. Lett.* **1996**, *25*, 933–934; b) L. Westerheide, F. K. Müller, R. Than, B. Krebs, J. Dietrich, S. Schindler, *Inorg. Chem.* **2001**, *40,* 1951–1961; c) R. H. Laye, F. K. Larsen, J. Overgaard, C. A. Muryn, E. J. L. McInnes, E. Rentschler, V. Sanchez, S. J. Teat, H. U. Güdel, O. Waldmann, G. A. Timco, R. E. P. Winpenny, *Chem. Commun.* **2005**, 1125–1127; d) Y. Miyazato, M. Ohba, S. Hayami, Y. Maeda, M. Tadokoro, H. Okawa, *Chem. Lett.* **2009**, *38*, 24–25; e) C. J. Reed, T. Agapie, *Inorg. Chem.* **2017**, *56*, 13360–13367.

[46] Metal/organic iron(II) complexes with bridging fluoro ligands: a) Y. Zang, H. G. Jang, Y.-M. Chiou, M. P. Hendrich, L. Que jr., *Inorg. Chim. Acta* **1993**, *213*, 41–48; b) S. Herold, L. E. Pence, S. J. Lippard, *J. Am. Chem. Soc.* **1995**, *117*, 6134–6135; c) S. Herold, S. J. Lippard, *Inorg. Chem.* **1997**, *36*, 50–58; d) J. Vela, J. M. Smith, Y. Yu, N. A. Ketterer, C. J. Flaschenriem, R. J. Lachicotte, P. L. Holland, *J. Am. Chem. Soc.* **2005**, *127*, 7857–7870; e) D. L. Reger, A. E. Pascui, M. D. Smith, J. Jezierska, A. Ozarowski, *Inorg. Chem.* **2012**, *51*, 11820–11836; f) S. Dammers, T. P. Zimmermann, S. Walleck, A. Stammler, H. Bögge, E. Bill, T. Glaser, *Inorg. Chem.* **2017**, *56*, 1779–1782; g) N. M. Hein, F. S. Pick, M. D. Fryzuk, *Inorg. Chem.* **2017**, *56*, 14513−14523; h) K. J. Anderton, B. J. Knight, A. L. Rheingold, K. A. Abboud, R. García-Serres, L. J. Murray, *Chem. Sci.* **2017**, *8*, 4123–4129; i) F. Jiang, M. A. Siegler, E. Bouwman, *Inorg. Chem. Commun.* **2018**, *94*, 53–56.

[47] F.-Q. Liu, H. Gornitzka, D. Stalke, H. W. Roesky, *Angew. Chem. Int. Ed.* **1993**, *32*, 442–444; *Angew. Chem.* **1993**, *105*, 447–448; b) F.-Q. Liu, A. Kunzel, A. Herzog, H. W. Roesky, M. Noltemeyer, R. Fleischer, D. Stalke, *Polyhedron* **1997**, *16*, 61–65; c) B. G. Harvey, A. M. Arif, A. Glöckner, R. D. Ernst, *Organometallics* **2007**, *26*, 2872–2879.

[48] M. Rancan, G. N. Newton, C. A. Muryn, R. G. Pritchard, G. A. Timco, L. Cronin, R. E. P. Winpenny, *Chem. Commun.* **2008**, 1560–1562.

[49] See *eg* a) T. Mahenthirarajah, P. Lightfoot, *Chem. Commun.* **2008**, 1401–1403; b) T. Mahenthirarajah, Y. Li, P. Lightfoot, *Dalton Trans.* **2009**, 3280–3285; c) H. Lin, P. A. Maggard, *J. Chem. Cryst.* **2011**, *41*, 1552–1559; d) V. Bulicanu, K. S. Pedersen, M. Rouzières, J. Bendix, P. Dechambenoit, R. Clérac, E. A. Hillard, *Chem. Commun.* **2015**, *51*, 17748–17751; e) K.-J. Chen, J. J. Perry, H. S. Scott, Q.-Y. Yang, M. J. Zaworotko, *Chem. Sci.* **2015**, *6*, 4784–4789; f) M. Lusi, P. B. A. Fechine, K.-J. Chen, J. J. Perry, M. J. Zaworotko, *Chem. Commun.* **2016**, *52*, 4160-4162.

[50] a) D. F. Evans, J. Chem. Soc. **1959**, 2003–2005; b) E. M. Schubert*, J. Chem. Educ.* **1992**, *69*, 62.

[51] C. J. O'Connor, *Prog. Inorg. Chem.* **1982**, *29*, 203–283.

[52] B. García, J. C. Ortega, *J. Chem. Eng. Data* **1988**, *33*, 200–204.

[53] *SIGMAPLOT*, v. 8.02; SPSS Scientific Inc., Chicago IL, USA, 2002.

[54] G. M. Sheldrick, *Acta Cryst. Sect. C: Struct. Chem.* **2015**. *71*, 1–8.

[55] L. J. Barbour, *J. Supramol. Chem.* **2001**, *1*, 189–191.

[56] O. V. Dolomanov, L. J. Bourhis, R. J. Gildea, J. A. K. Howard, H. Puschmann, *J. Appl. Crystallogr.* **2009**, *42*, 339–341.

[57] I. D. Brown, Bond valence parameters. https://www.iucr.org/resources/data/data-sets/bond-valence-parameters.